Quantum chemical study of the coordination of glycolic acid conformers and their conjugates to [Ca(OH2)n]2+ (n = 0–4) ions

ARTICLE *in* JOURNAL OF MOLECULAR STRUCTURE THEOCHEM · JULY 2003

Impact Factor: 1.37 · DOI: 10.1016/S0166-1280(03)00148-9

3 AUTHORS, INCLUDING:

Athanassios C Tsipis
University of Ioannina
48 PUBLICATIONS **969** CITATIONS
SEE PROFILE

Vicky Valla
Aristotle University of Thessaloniki
8 PUBLICATIONS **98** CITATIONS
SEE PROFILE

ELSEVIER

Journal of Molecular Structure (Theochem) 630 (2003) 81–100

THEO CHEM

www.elsevier.com/locate/theochem

Quantum chemical study of the coordination of glycolic acid conformers and their conjugate bases to $[Ca(OH_2)_n]^{2+}$ ($n = 0-4$) ions

Athanassios C. Tsipis, Constantinos A. Tsipis*, Vicky Valla

Laboratory of Applied Quantum Chemistry, Faculty of Chemistry, Aristotle University of Thessaloniki, 540-06 Thessaloniki, Greece

Received 7 August 2002; accepted 15 November 2002

Abstract

A detailed exploration of the configurational and conformational space of glycolic acid and their conjugate bases has been carried out with the aid of first principles quantum chemical techniques at the B3LYP/6-311 + G(d,p) and CCSD(T)/6-31G(d,p) levels of theory. The most stable configuration among the eight possible glycolic acid conformers corresponds to the *E-s-cis*, *s-trans* configuration, while the highest energy *E-s-trans*, *s-cis* conformer was found at 10.88 and 12.17 kcal mol^{-1} higher in energy at the B3LYP/6-311 + G(d,p) and CCSD(T)/6-31G(d,p) levels of theory, respectively. Upon dissociation of glycolic acid the *s-cis*(*syn*), and *s-trans*(*anti*) configurations of the glycolate anion can be formed. The *anti* conformer was found to be less stable than the *syn* one by 14.20 and 16.87 kcal mol^{-1} at the B3LYP/6-311 + G(d,p) and CCSD(T)/6-31G(d,p)) levels of theory, respectively. The computed B3LYP/6-311 + G(d,p) proton affinity of the *syn* conformer for the protonation process affording the more stable *E-s-cis*, *s-trans* conformer, in vacuum was found to be 325.35 kcal mol^{-1} (ΔG^0 value). From a methodological point of view, our results confirm the reliability of the integrated computational tool formed by the B3LYP density functional model. This model has subsequently been used to investigate the interaction of Ca^{2+} ions with the glycolic acid conformers and their conjugate bases in vacuum and in the presence of extra water ligands. For the complexes of glycolic acid conformers the η^2–O,O–(C**O**OH) coordination, that is the structure that arises from the coordination of the Ca^{2+} to the carboxylic group, is the global minimum of the PES, while the η^2–O(**O**H),O–(CO**O**H) coordination is a local minimum found at only 1.0 and 1.3 kcal mol^{-1} higher in energy at the B3LYP/6-311 + G(d,p) and CCSD(T)/6-31G(d,p) levels of theory, respectively. Moreover, the two isomers exhibit nearly the same binding affinities, which are predicted to be 89 and 85 kcal mol^{-1} at the B3LYP/6-311 + G(d,p) and CCSD(T)/6-31G(d,p) levels of theory, respectively. The same holds also true for the complexes of the glycolate anion. The η^2–O,O–(C**O**O$^-$) coordination involving the *syn* conformer of the glycolato ligand, is the global minimum, while the η^2–O(**O**H),O–(C**O**O$^-$) one lies at 1.5 and 5.6 kcal mol^{-1} higher in energy at the B3LYP/6-311 + G(d,p) and CCSD(T)/6-31G(d,p) levels of theory, respectively. The other conformer with an η^2–O,O–(C**O**O$^-$) coordination involving the *anti* conformer of the glycolato ligand, is less stable by only 0.2 kcal mol^{-1} at both levels of theory. Noteworthy is the trend seen for the incremental binding energy due to the successive addition of water molecules to $[HOCH_2C(O)O]Ca^{2+}$ species; the computed values are 30.4, 26.8, 22.9 and 16.2 kcal mol^{-1} at the B3LYP/6-311 + G(d,p) level of theory for the mono-, di-, tri- and tetraaqua complexes, respectively. This trend arising from the repulsion of the dipoles between the water ligands and from unfavorable many body interactions is in accordance with those anticipated from electrostatic considerations. The Ca(II)-water interaction weakens with increasing coordination of the metal. Obviously, it is

* Corresponding author. Tel.: +23-10-997851.
E-mail address: tsipis@chem.auth.gr (C.A. Tsipis).

doi:10.1016/S0166-1280(03)00148-9

the electrostatic nature of the Ca(II)-water interactions that accounts well for the computed coordination geometries of the cationic (aqua)(glycolato)calcium complexes. Calculated structures, relative stability and bonding properties of the conformers and their complexes with $[Ca(OH_2)_n]^{2+}$ ($n = 0-4$) ions are discussed with respect to computed electronic and spectroscopic properties, such as charge density distribution, harmonic vibrational frequencies and NMR chemical shifts.

Keywords: Density functional theory; Glycolic acid; Glycolato ligand; Glycolatocalcium complexes; (Aqua)(glycolato)calcium complexes

1. Introduction

Interactions between divalent metal ions and biomolecules are common both in solution and in the gas phase. In the last few years, both experimental and theoretical techniques have been employed to quantify these interactions in simpler systems, ionized amino acids in the gas phase [1–4]. Despite the importance of divalent metal ion interactions with biomolecules both in solution and in the gas phase only recently the intrinsic structure of glycine in the absence of solvent has been studied at the density functional theory (DFT) and Moller-Plesset levels of theory. The results indicated that the divalent metal ions dramatically influence the structure of the simplest amino acid glycine in the gas phase.

Previous theoretical studies have analyzed the interaction of alkali [3–6] and alkaline earth metal cations [7,8], nickel mono-cation [8], copper mono- and di-cation [8–10] with glycine. These studies focus on the bonding and relative energies of the different chelating structures as well as on the study of the intramolecular proton transfer reactions relating the neutral and zwitterionic structures of the amino acid, which show different behavior in many biochemical processes. The interaction energies of functional groups representing the side chains of amino acid residues with Co^{2+}, Ni^{2+}, Cu^{2+}, Zn^{2+}, Cd^{2+}, and Hg^{2+} cations were recently [11] reported using the DFT/B3LYP method. Moreover, the reactions between formic acid (or glycine) and ammonia, without and with Mg, Ni and Cu cations as catalysts, have been studied as model reactions for peptide bond formation using the B3LYP/6-311 + G(d,p) method [12]. Despite the importance of calcium in the biological systems, the structure and energy of glycine bound to calcium divalent cations has recently been determined at the B3LYP and local MP2 levels of theory using effective core potentials of Hay and Wadt for Ca and the LACVP + (d,p) basis set [8].

The biochemistry of calcium has always been very intriguing for the scientific community. The calcium-dependent metabolic pathways are constantly increasing as its study attracts more and more scientists. The central controls of calcium involve the light harvesting and coupling to photosynthesis of dioxygen, the control of dehydrogenases in oxidative phosphorylation as well as multiple kinase reactions. In addition, calcium is involved in the control of the mechanical stability of the walls of the cells, in the muscle contraction, in fertilization, in cell division and in plentiful hormonal activities. The wealth of its activity is due to the size and electronic configuration of calcium dications, which allow them to coordinate with a variety of functional groups in biological molecules. On the other hand, there are a number of skin cream and lotions on the market today that contain α-hydroxy acids such as glycolic acid $HOCH_2COOH$. These acids dissolve the older rougher skin cells leaving behind younger skin cells.

In this paper, we explore the conformational space of glycolic acid and its conjugate base as well as their associations with $[Ca(OH_2)_n]^{2+}$ ($n = 0-4$) ions using the DFT at the B3LYP/6-311 + G(d,p) level pursuing a three-fold objective: (i) the determination of the ground states, structures, relative stabilities and spectroscopic properties (IR, NMR) of the complexes, (ii) the understanding of the bonding properties of the complexes using a variety of theoretical analysis techniques, which include electron topology properties, natural bond orbital (NBO) and Mulliken population analysis, (iii) the unveiling of the similarities and differences in the coordination modes of glycolic acid conformers and their conjugate bases towards calcium dications.

2. Computational details

Standard ab initio molecular orbital theory [13] and DFT [14] were carried out using the GAUSSIAN 98 program suite [15]. The geometries were fully optimized at the Becke's 3-Parameter hybrid functional combined with the Lee-Yang-Parr correlation functional abbreviated as B3LYP level of density functional theory, using the polarized triple zeta split valence 6-311 + G(d,p) basis set. Moreover, single-point energy calculations used the single and double excitation coupled cluster method with a perturbational estimate of the triple excitations CCSD(T) method combined with the smaller 6-31G(d,p) basis set. In all computations no constrains were imposed on the geometry. Full geometry optimization was performed for each structure using Schlegel's analytical gradient method [16], and the attainment of the energy minimum was verified by calculating the vibrational frequencies that result in absence of imaginary eigenvalues. All the stationary points have been identified for minimum (number of imaginary frequencies NIMAG = 0) or transition states (NIMAG = 1). The vibrational modes and the corresponding frequencies are based on a harmonic force field. This was achieved with the SCF convergence on the density matrix of at least 10^{-9} and the rms force less than 10^{-4} a.u. All bond lengths and bond angles were optimized to better than 0.001 Å and 0.1°, respectively. The computed electronic energies were corrected to constant pressure and 298 K, for zero point energy (ZPE) differences. Magnetic shielding tensors have been computed with the GIAO (gauge-including atomic orbitals) DFT method [17] as implemented in the GAUSSIAN 98 series of programs [15] employing the B3LYP level of theory.

3. Results and discussion

3.1. Conformations of glycolic acid and its conjugate base in the gas phase

Glycolic acid and its conjugate base can exist in the conformations *s-cis*(*syn*) and *s-trans*(*anti*) with respect to the C–OH and C(O)–OH single bonds. The eight stationary points located on the potential energy surface (PES) of glycolic acid along with their structural parameters computed at the B3LYP/6-311 + G(d,p) level of theory are shown in Fig. 1. The absolute and relative energies, dipole moments μ and hardness η of glycolic acid and its conjugate base conformers computed at the B3LYP/6-311 + G(d,p) and CCSD(T)/6-31G(d,p) levels of theory are given in Table 1.

3.1.1. Calculated structures and stability

Perusal of Fig. 1 illustrates that the global minimum in the PES of glycolic acid corresponds to the *E-s-cis*, *s-trans* conformer, **1** at both the B3LYP/6-31G(d,p) and the CCSD(T)/6-31G(d,p) levels of theory. Moreover, two of the stationary points exhibiting the *Z-s-cis*, *s-trans*, **2TS** and *Z-s-trans*, *s-trans*, **5TS** correspond to saddle points on the PES at 1.98(3.00) and 4.19(5.15) kcal mol^{-1} higher in energy than the more stable *E-s-cis*, *s-trans* conformer at the B3LYP/6-311 + G(d,p) and CCSD(T)/6-31G(d,p) (figures in parentheses) level of theory. Notice that at the correlated CCSD(T)/6-31G(d,p) level the computed energy values are about 1 kcal mol^{-1} higher than the B3LYP/6-311 + G(d,p) ones. All conformers, except **2TS** and **4**, adopt planar geometries. The **2TS** and **5TS** conformers possess one imaginary frequency, thereby being the transition states for possible *s-cis*, *s-trans* isomerization processes of the conformers with a *Z*-configuration. Interestingly, conformer **2TS** with a non-planar geometry is less stable than the planar one corresponding to the local minimum **3** by about 1 kcal mol^{-1} only at the correlated CCSD(T)/6-31G(d,p) level. The H atom of the H–O–C– moiety was found out of the molecular plane, with the H–O–C–C dihedral angle being 46.5°. The highest energy conformer **8** of glycolic acid, exhibiting the *E-s-trans*, *s-cis* configuration corresponds to local minimum on the PES at 10.88(12.17) kcal mol^{-1} higher in energy than the more stable *E-s-cis*, *s-trans* isomers **1** at the B3LYP/6-311 + G(d,p)(CCSD(T)/6-31G(d,p)) levels of theory. Generally, the C–OH, C–C, C=O and C(O)–OH bond lengths were found in the expected regions of 1.405–1.428, 1.513–1.528, 1.191–1.207 and 1.342–1.365 Å, respectively. The C–OH and C(O)–OH bonds are predicted to be more sensitive to conformational changes than the C–C and C=O ones. Moreover, in conformers **1**, **2TS**, **3**, **4** and **7**

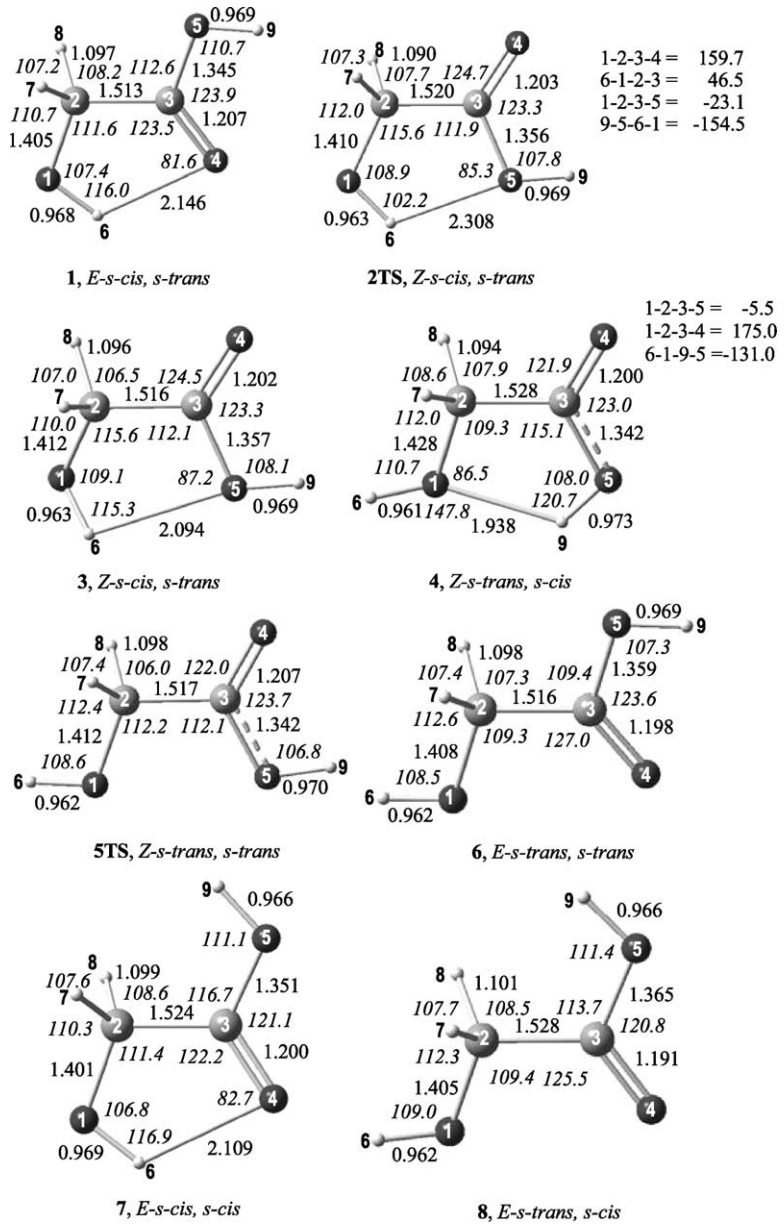

Fig. 1. Equilibrium structures (bond lengths in Å, bond angles in degrees), of glycolic acid conformers, computed at the B3LYP/6-311 + G(d,p) level of theory.

the computed H···O distances found in the range of 1.938–2.308 Å suggest the formation of intramolecular H-bonds [18]. The shortest H···O distance was predicted to be that between the H atom of the carboxylic group and the O atom of the hydroxylic group and corresponds to the higher value of the ∠O–H···O bond angle of 120.7°. In general terms the optimized geometry of the more stable conformer **1** is in excellent agreement with the experimental structure determined by microwave spectrometry [19]. The experimentally determined C–OH, C–C, C=O, C(O)–OH, C–H, CO–H and

Table 1
Absolute (a.u.) and relative energies (in kcal mol^{-1}), dipole moments μ (in D) and hardness η (in eV) of glycolic acid and its conjugate base conformers computed at the B3LYP/6-311 + G(d,p) and CCSD(T)/6-31G(d,p)//B3LYP/6-311 + G(d,p) levels of theory

Conformer	B3LYP		CCSD(T)//B3LYP		μ	η
	$E_{abs.}$	E_{rel}	E_{abs}	E_{rel}		
E-s-cis-s-trans, **1**	− 304.329269	**0.00**	− 303.526004	**0.00**	2.41(2.44)[a]	3.682(8.523)
Z-s-cis-s-trans, **2TS**	− 304.326119	1.98	− 303.521218	3.00	1.67(1.74)	3.719(8.490)
Z-s-cis-s-trans, **3**	− 304.325754	2.20	− 303.522700	2.07	1.92(2.03)	3.586(8.347)
Z-s-trans-s-cis, **4**	− 304.324601	2.93	− 303.519992	3.77	5.10(5.45)	3.555(8.394)
E-s-cis-s-trans, **5TS**	-304.322595	4.19	− 303.517791	5.15	1.78(1.91)	3.841(8.604)
E-s-cis-s-trans, **6**	− 304.322209	4.34	− 303.518530	4.69	3.25(3.42)	3.853(8.626)
E-s-cis-s-trans, **7**	− 304.320833	5.29	− 303.516451	5.99	3.55(3.75)	3.760(8.624)
E-s-cis-s-trans, **8**	− 304.311926	10.88	− 303.506614	12.17	5.86(6.23)	3.638(8.480)
s-cis, **9**	− 303.802430	**0.00**	− 302.958222	**0.00**	2.96(3.12)	2.795(8.329)
s-trans, **10**	− 303.779791	2.93	− 302.931332	3.77	6.24(6.47)	2.195(7.245)

[a] Figures in parentheses are the computed CCSD(T)//B3LYP values.

C(O)O–H bond lengths are 1.406, 1.495, 1.210, 1.349, 1.097, 0.956 and 0.989 Å, respectively [19]. Moreover, the experimental values of the ∠H(6)–O(1)–C(2), ∠O(1)–C(2)–C(3), ∠C(2)–C(3)–O(4), ∠C(2)–C(3)–O(5), ∠O(4)–C(3)–O(5) and ∠C(3)–O(5)–H(9) bond angles are 105.2, 111.3, 124.2, 112.6, 123.2 and 105.5°, respectively (the atomic numbering scheme refers to Fig. 1).

Upon dissociation of glycolic acid two possible conformers of the glycolate anion, namely the *s-cis*(*syn*), **9** and *s-trans*(*anti*), **10** can be formed. The structural parameters of the glycolate anion conformers computed at the B3LYP/6-311 + G(d,p) level of theory, along with the relative stability, dipole moments μ and hardness η computed at the B3LYP/6-311 + G(d,p) and CCSD(T)/6-31G(d,p) levels of theory are given in Fig. 2. The *anti* conformer was found to be less stable than the *syn* conformer by 14.20(16.87) kcal mol^{-1} at the B3LYP/6-311 + G(d,p)(CCSD(T)/6-31G(d,p)) levels of theory. The stabilization of the *syn* conformer is attributed to the intramolecular H-bond formation. The computed B3LYP/6-311 + G(d,p) proton affinity of the *syn* conformer for the protonation process affording the more stable *E-s-cis*, *s-trans* conformer, **1** in the gas phase was found to be 325.35 kcal mol^{-1} (ΔG^0 value). This value is in line with the CBS-QB3, G2, G2MP2 and G3 ΔG^0 values of 329.1, 328.8, 329.2

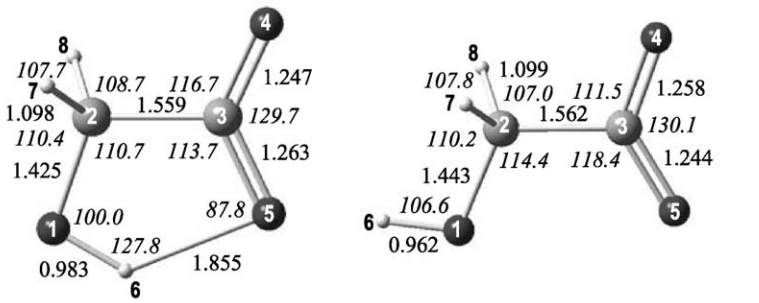

9, *s-cis*
ΔE = 0.00(0.00) kcal mol^{-1}
μ= 2.96(3.12) D, η = 2.795(8.329) eV

10, *s-trans*
ΔE =14.20(16.87) kcal mol^{-1}
μ= 6.24(6.47) D, η = 2.195(7.245) eV

Fig. 2. Equilibrium structures (bond lengths in Å, bond angles in degrees), relative stability (in kcal mol^{-1}), dipole moments and hardness of glycolate anion conformers computed at the B3LYP/6-311 + G(d,p) level of theory. Figs. in parentheses are the relative energies, dipole moments and hardness computed at the CCSD(T)/6-31G(d,p)//B3LYP/6-311 + G(d,p) level of theory.

and 329.5 kcal mol^{-1}, respectively for chloroacetic acid in the gas phase reported recently [20].

The glycolic acid dissociation results in a few structural changes, which are more pronounced on the carboxylate group. Thus, the two C–O bonds in the ionized carboxylate group become almost equivalent (C–O bond length of 1.24–1.26 Å) acquiring an intermediate character between the C=O and C–OH bonds of the carboxylic group accompanied by opening of the ∠OCO bond angle by about 7° as well. In addition both the C–C and C–OH bonds are lengthened upon dissociation of the acid. More characteristic is the shortening of the H-bond distance in the conjugate base of glycolic acid by 0.2–0.3 Å, probably as a result of the increased negative net atomic charge acquired by the O atoms of the ionized carboxylate group.

3.1.2. Electronic properties and bonding

The HOMOs (Highest Occupied Molecular Orbitals) of glycolic acid conformers (except TSs) correspond to an antibonding combination of the two σ bonding MOs located on the C–H bonds of the CH_2 moiety in conjunction with a strong non-bonding component with p character located on the O atom of the alcoholic hydroxylic group (Fig. 3). Obviously, any electrophilic attack of the glycolic acid conformers would take place on the C atom of the CH_2OH group. On the other hand, the HOMO of the conjugate bases corresponds to a non-bonding MO localized on the carboxylate group with its components being p-type wavefunctions of the two O atoms in an out-of-phase combination. The nature of the HOMO suggests that both O atoms of the ionized carboxylate group are the nucleophilic centers of the conjugate bases. The LUMOs (Lowest Unoccupied Molecular Orbitals) of glycolic acid conformers (except TSs) correspond to a π^* antibonding MO spanning mainly the nuclear skeleton of the carboxylate moiety, being thus the nucleophilic center of the molecules. The LUMO of the conjugate bases are non-bonding orbitals located primarily on the H atoms of the CH_2 moiety thereby any nucleophilic attack of the conjugate bases would take place on the CH_2 croup. The HOMO–LUMO energy gap of the glycolic acid conformers is higher than that of their conjugate bases. Notice that the hardness η (Figs. 1 and 2), of the conformers defined by Parr and Pearson [21] as $\eta = 1/2(\mathrm{IP} - \mathrm{EA}) = 1/2(\epsilon_{\mathrm{LUMO}} - \epsilon_{\mathrm{HOMO}})$, where *IP* and *EA* are the first vertical ionization potential and electron affinity of the species, which in the framework of Koopman's theorem can be approximated by ϵ_{HOMO} and ϵ_{LUMO} with opposite sign, respectively predicts the most stable conformer of the conjugate bases, but fails to predict the relative stability of the undissociated glycolic acid conformers.

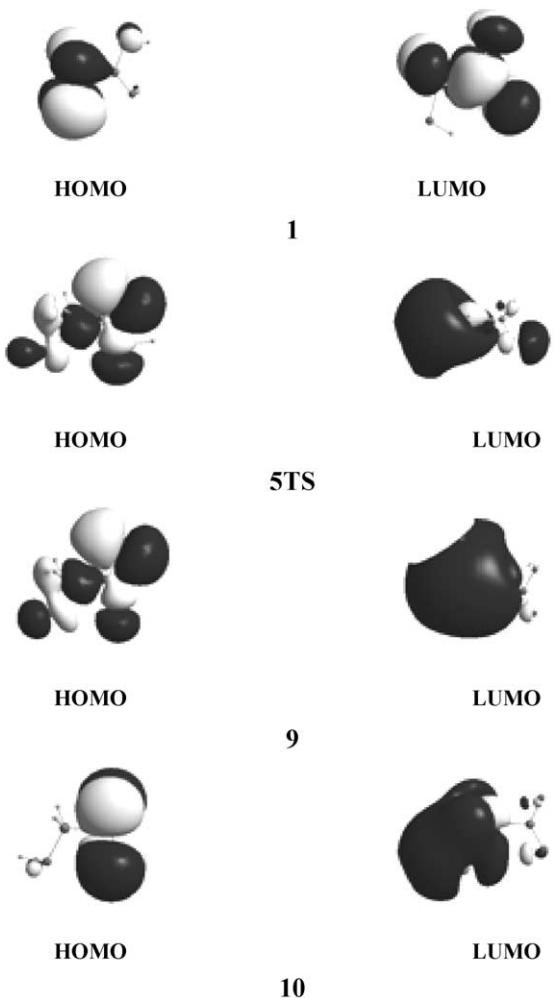

Fig. 3. HOMO (Highest Occupied Molecular Orbital) and LUMO (Lowest Unoccupied Molecular Orbital) of selected conformers of glycolic acid and glycolate anion.

The Mulliken and NBO population analysis (net atomic and natural charges q and bond overlap

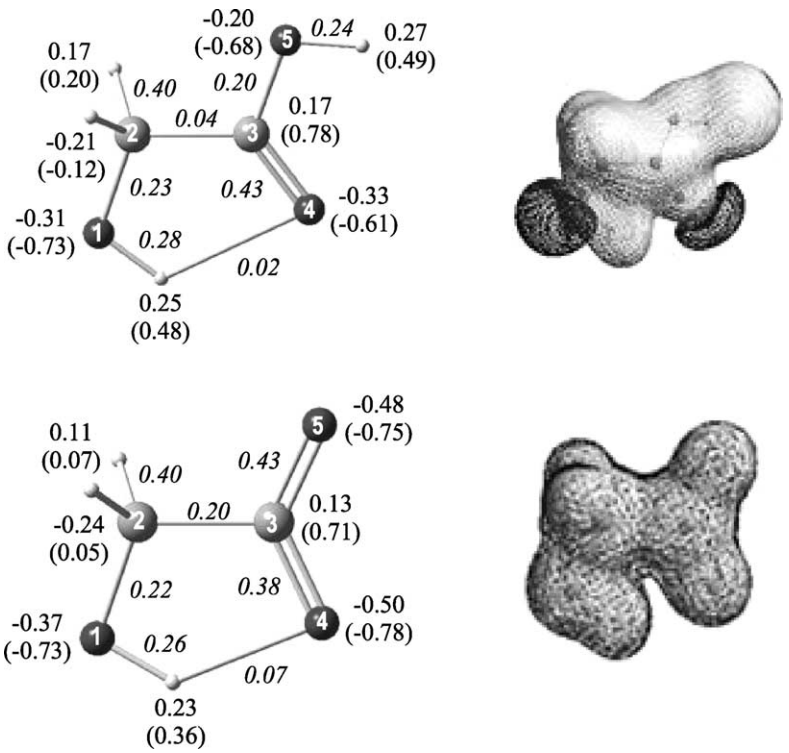

Fig. 4. The Mulliken and NBO population analysis along with the MEP (isopotential surfaces of 1.00 a.u.) of the more stable conformers of glycolic acid, **1** and its conjugate base **9** computed at the B3LYP/6-311 + G(d,p) level of theory. Natural charges are given in parentheses and bond overlap population values in italics.

population, bop) of the more stable conformers of glycolic acid, **1** and its conjugate base **9** computed at the B3LYP/6-311 + G(d,p) level are shown in Fig. 4. The Mulliken net atomic charges and bops for all conformers computed at the B3LYP/6-311 + G(d,p) level of theory are listed in detail in the Supporting Information (Table S1). The molecular electrostatic potentials (MEP) of **1** and **9** are also depicted schematically in Fig. 4. It can be seen that there are no significant changes on both net atomic charges and natural charges in the glycolic acid conformers. It is worth to be noted that the C–O**H** and C(O)O**H** hydrogen atoms acquire nearly the same positive net atomic (natural) charges of 0.25–0.28 (0.46–0.48) charge units. The computed C–**O**–**H** and C(O)**O**–**H** bond overlap population (bop) values were found in the range of 0.19–0.24 and 0.20–0.30, respectively. In general terms, with the exception of conformers **6** and **4** the bop values for the C–**O**–**H** bond are higher than those of the C(O)**O**–**H** one. This observation strongly suggests that, in spite of nearly the same positive charge of the C–O–**H** and C(O)O–**H** hydrogen atoms, the latter could be dissociated more easy than the former one. The computed O–H···O bop values of 0.02 and 0.07 a.u. for glycolic acid and its conjugate base, respectively, reveal the formation of hydrogen bond being more pronounced in the conjugate base, because of the higher negative charge on the O atom. Finally, proton dissociation does not alter significantly the electrostatic potential map of the glycolate anion.

3.1.3. Infrared spectra

We only analyze the infrared spectra of the more stable conformer, **1**, and its conjugate base **9** as most of the computed harmonic vibrational frequencies and the corresponding normal modes are not sensitive to configurational and conformational changes. Selected harmonic vibrational frequencies and the corresponding normal modes for all conformers at

Table 2
The computed GIAO-B3LYP ^{13}C, ^{17}O and ^{1}H chemical shifts (δ, ppm) of glycolic acid conformers and its conjugate bases using the 6-311 + G(d,p) basis sets

Conformer	$^{17}O(1)$	$^{13}C(2)$	$^{13}C(3)$	$^{17}O(4)$	$^{17}O(5)$	$^{1}H(6)$	$^{1}H(7,8)$	$^{1}H(9)$
E-s-cis-s-trans, **1**	9.6	69.2	188.8	399.0	191.4	1.7	4.3	6.0
Z-s-cis-s-trans, **2TS**	12.6	72.4	182.8	404.8	199.2	1.3	4.4	5.9
Z-s-cis-s-trans, **3**	23.9	73.2	183.7	408.8	201.6	0.9	4.4	5.9
Z-s-trans-s-cis, **4**	21.7	72.1	178.3	411.0	194.5	1.0	4.1	8.8
Z-s-trans-s-trans, **5TS**	18.0	72.2	183.3	399.5	209.8	0.1	4.4	6.0
E-s-trans-s-trans, **6**	15.7	69.5	188.5	422.6	194.7	0.0	4.4	5.6
E-s-cis-s-cis, **7**	12.5	69.7	186.8	415.3	193.4	1.9	4.0	5.6
E-s-trans-s-cis, **8**	18.8	69.6	175.7	441.8	192.3	0.2	4.1	5.0
s-cis, **9**	36.2	76.4	184.4	312.8	298.0	3.8	3.3	
s-trans, **10**	34.4	74.3	179.3	300.3	330.0	−1.1	3.8	

The calculated absolute ^{13}C, ^{17}O and ^{1}H shielding tensor elements σ^{iso} (σ^{aniso}) for CH_4, H_2O and TMS external reference standards at the same level of theory are 190.4(0.1), 322.6(51.3) and 32.0(9.2), respectively.

the B3LYP/6-311 + G(d,p) level of theory are listed in detail in the Supporting Information (Table S2). The two high frequency normal modes in the regions of 3756–3863 and 3674–3795 cm^{-1} could be assigned to ν(O–H) stretching vibrations of the C–OH and C(O)–OH moieties, the former absorbing at higher frequencies. In the conjugate base **9** involving H-bond the ν(O–H) stretching vibration is shifted to much lower wave numbers (3461 cm^{-1}). The same is also true for the conformers involving H-bond showing the lower ν(CO–H) stretching vibrations. The relatively strong ν(C=O) stretching vibration of the glycolic acid conformers is predicted to occur in the region of 1806–1882 cm^{-1}. Upon proton dissociation this band is shifted to lower frequencies (1683 cm^{-1}) as a result of the electron density delocalization on the C(O)O moiety of the conjugate base resulting in C–O bonds with a partial double bond character. Finally, in the region of 1023–1167 cm^{-1} the relatively strong IR bands ascribable to ν(C–O) stretching vibrations are predicted to occur. These bands are also shifted to lower frequencies upon ionization of the acid.

3.1.4. NMR spectra

Employing gradient-corrected levels of DFT ^{13}C, ^{17}O and ^{1}H chemical shifts were calculated at the GIAO/B3LYP/6-311 + G(d,p) level of theory using the B3LYP/6-311 + G(d,p) optimized geometries. The computed ^{13}C, ^{17}O and ^{1}H chemical shifts (δ, ppm) of glycolic acid conformers and their conjugate bases, as the difference between the shielding of the reference and the shielding of the molecule of interest, $\delta = \sigma_{ref} - \sigma$ are summarized in Table 2. The absolute isotropic shielding tensor elements for the CH_4, NH_3 and H_2O molecules used as external reference standards in the gas phase NMR are also given in Table 2.

The computed $^{13}C(2)$ chemical shifts of the glycolic acid conformers and their conjugate bases found in the range of 69.2–76.4 ppm are in good agreement with the experimental values of 62.39 ppm [22]. On the other hand, the carboxylic $^{13}C(3)$ chemical shifts found in the range of 175.7–188.8 ppm are also in line with available experimental data (180.72 ppm) [22].

The $^{17}O(COH)$ chemical shifts of the alcoholic O atom of glycolic acid conformers were found in the range of 9.6–23.9 ppm. For the conjugate bases the $^{17}O(COH)$ chemical shifts are moved to higher fields (36.2–34.4 ppm). The $^{17}O(C(O)OH)$ chemical shifts of the hydroxylic oxygen atom of the carboxylic group of glycolic acid conformers were found in the region of 191.4–209.8 ppm. In the conjugate bases there is a strong shielding effect and the $^{17}O(C(O)OH)$ chemical shifts are shifted to higher fields (298.0–330.0 ppm) as a result of the electron density accumulation on these oxygen atoms. On the other hand, the $^{17}O(C=O)$ chemical shifts of the carbonyl oxygen atom of the carboxylic group of glycolic acid conformers found at much higher magnetic fields (399.0–441.8 ppm) are deshielded upon ionization of

the acids (300.3–312.8 ppm) since the π electron density is delocalized over the carboxylate C(O)O moiety.

The ^{1}H(CO*H*) chemical shifts of the glycolic acid conformers were found in the region of 0.2–1.9 ppm. In the conjugate bases **9** and **10** the ^{1}H(CO*H*) chemical shifts were found at 3.8 and −1.1 ppm, respectively. On the other hand, the ^{1}H(C(O)O*H*) chemical shifts of the glycolic acid conformers were found in the range of 5.0–8.8 ppm. Finally, the ^{1}H(*H*2C) chemical shifts found in the range of 3.3–4.4 ppm are characteristic of ^{1}H NMR chemical shifts of hydrogen atoms bound to nearly sp^3-hybridized carbon atoms and are in excellent agreement with the experimental value of 4.13 ppm [22].

3.2. Coordination of glycolic acid conformers and their conjugate bases to $[Ca(H_2O)_n]^2$ (n0–4) ions

The interaction of Ca^{2+} ions with the glycolic acid conformers and their conjugate bases in the gas phase and in the presence of extra water ligands was analyzed in the framework of DFT theory. There are three electron-rich binding sites (the three O donor atoms) in glycolic acid and glycolate ligands, thereby they could be coordinated to Ca^{2+} ion according to the following bonding modes: (i) through the O donor atoms of the carboxylic or carboxylato group either in a monodentate or bidentate coordination mode and (ii) through the alcoholic O donor atom and one of the O donor atoms of the carboxylic or carboxylato group forming a five-membered chelate ring.

3.2.1. Calculated structures, relative stabilities and bonding of $[HOCH_2C(O)OH]Ca^{2+}$, and $[HOCH_2C(O)O]Ca^+$ complexes

The equilibrium structures of $[HOCH_2C(O)OH]Ca^{2+}$ and $[HOCH_2C(O)O]Ca^+$ complexes corresponding to global and local minima in the PES along with the relative stability and dipole moments computed at the B3LYP/6-311 + G(d,p) and CCSD(T)/6-31G(d,p) levels of theory are shown in Fig. 5. The computed interaction energies of the Ca^{2+} ions with glycolic acid conformers and their conjugate bases for selected bonding modes are collected in Table 3. Notice that, as it is generally found [10,22] the B3LYP binding affinities are larger than the ones computed using conventional post-Hartree–Fock methods. For the complexes of glycolic acid conformers the η^2–O,O–(C**OO**H) coordination **11**, that is the structure that arises from the coordination of the Ca^{2+} to the carboxylic group, is the global minimum of the PES, while the η^2–O(**O**H),O–(CO**O**H) coordination **12** is a local minimum found at only 1.0 and 1.3 kcal mol^{-1} higher in energy at the B3LYP and CCSD(T) levels of theory, respectively. Moreover, the two isomers exhibit nearly the same binding affinities, which are predicted to be 89 and 85 kcal mol^{-1} at the B3LYP and CCSD(T) levels of theory, respectively. The same holds also true for the complexes of the glycolate anion. The η^2–O,O–(C**OO**$^-$) coordination **13** involving the glycolate ligand **9**, is the global minimum, while the η^2–O(**O**H),O–(C**O**O$^-$) one **15** lies at 1.5 and 5.6 kcal mol^{-1} higher in energy at the B3LYP and CCSD(T) levels of theory, respectively. The other conformer with an η^2–O,O–(C**OO**$^-$) coordination **14** involving the glycolate ligand **10**, is less stable than **13** by only 0.2 kcal mol^{-1} at both levels of theory. The computed binding affinities of the $[HOCH_2C(O)O]Ca^+$ complexes are almost three times higher than those of $[HOCH_2C(O)OH]Ca^{2+}$ ones (Table 3) because of the higher negative charge on the O donor atoms of the anionic glycolate ligands, which strongly contributes to the increase of the electrostatic component of the metal-ligand interaction. It is worth noting that the interaction energies of the $[HOCH_2C(O)O]Ca^+$ complexes are comparable to those of the Cu^{2+}-glycine complexes computed at the same levels of theory [10].

The coordination of Ca^{2+} dication with the neutral and ionized forms of glycolic acid ligands leads to structural changes accompanied by significant charge redistributions as well. The net atomic charges and bops computed at the B3LYP/6-311G(d,p) level are given in Supporting Information (Table S3).

In the η^2–O,O–(C**OO**H) coordination **11**, the bonding mode of glycolic acid to Ca^{2+} ion is asymmetric, the two Ca–O bond distances are equal to 2.240 and 2.504 Å. The interaction of the Ca^{2+} with the carbonyl O donor atom of the carboxylic group exhibits a higher covalent component with respect to its interaction with the hydroxylic O donor atom. This is reflected on the Ca–O bop values of 0.16 and 0.06 a.u., respectively. Interestingly, there is also a week interaction of the Ca^{2+} dication with the C atom of

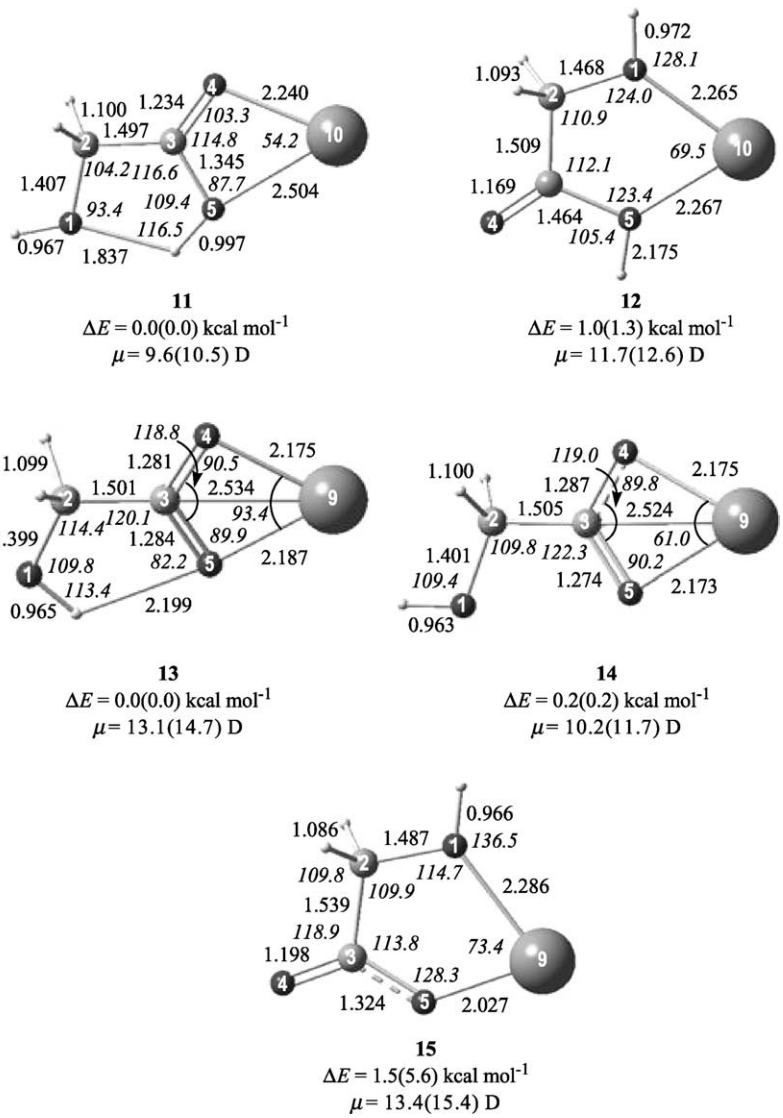

Fig. 5. Equilibrium structures (bond lengths in Å, bond angles in degrees), relative stability (in kcal mol^{-1}) and dipole moments of $[HOCH_2C(O)OH]Ca^{2+}$ and $[HOCH_2C(O)O]Ca^{+}$ complexes computed at the B3LYP/6-311 + G(d,p) level of theory. Figs. in parentheses are the relative energies and dipole moments computed at the CCSD(T)/6-31G(d,p)//B3LYP/6-311 + G(d,p) level of theory.

the carboxylic group corresponding to a bop value of 0.06. The association of Ca^{2+} dication with the glycolic acid results in the lengthening of the C=O bond by 0.034 Å with concomitant narrowing of the ∠O=C−O bond angle by about 8°. The C−O bond length is not altered and the H-bond becomes stronger upon coordination. The net atomic charge transferred to Ca^{2+} dication is 0.40 charge units. Most of the charge transferred comes from the C atom of the coordinated −COOH group, which acquires a positive net atomic charge of 0.34 charge units (compare with the value of 0.13 charge units in the free ligand). Interestingly, the O(H) donor atom directly involved in the bonding acquires a significantly higher negative net atomic charge of 0.15 charge units with respect to the free ligand. Notice that the natural population analysis predicts a much smaller charge transferred to Ca^{2+} ion of only 0.08

Table 3
Calculated binding affinities ΔH_0 (in kcal mol^{-1}) of the $[HOCH_2C(O)OH]Ca^{2+}$ and $[HOCH_2C(O)O]Ca^{2+}$ complexes at the B3LYP/6-311 + G(d,p) and CCSD(T)/6-31G(d,p) levels of theory

Compound	B3LYP	CCSD(T)
13	88.9(86.0)[a]	85.4(81.6)
14	89.3(85.1)	85.4(80.3)
15	301.8(301.8)	295.7(295.7)
16	315.8(301.6)	312.3(295.5)
17	314.5(300.3)	306.6(289.7)

[a] Figures in parentheses are the binding affinities with respect to the more stable conformer.

charge units. The natural electron configuration indicates that the mixing of metal s and d orbitals is responsible for the week covalent interaction of the Ca^{2+} dication with glycolic acid.

In the η^2–O(**O**H),O–(CO**O**H) coordination **12**, the bonding mode of glycolic acid to Ca^{2+} is symmetric, the two Ca–O bond distances being 2.265 and 2.267 Å. The interaction of the Ca^{2+} with both O donor atoms involves a week covalent component corresponding to a Ca–O bop value of only 0.08 a.u. The association of Ca^{2+} dication with glycolic acid results in the lengthening of both the C–O(H) and C(O)–O(H) bonds by 0.056 and 0.122 Å, which become nearly equivalent in the complex. The net atomic (natural) charge transferred to Ca^{2+} dication is 0.31 (0.07) charge units. Interestingly, both the C–**O**(H) and C(O)–**O**(H) coordinated O donor atoms acquire a significantly higher negative net atomic charge of 0.15 and 0.26 charge units, respectively with respect to the free ligand.

In the η^2–O,O–(C**OO**$^-$) coordination **14** the bonding mode of glycolato ligand to Ca^{2+} is symmetric (Ca–O bond distances of 2.173 and 2.175 Å). However, the H-bond formation in **13** introduces an asymmetry in the η^2–O,O–(C**OO**$^-$) bonding mode (Ca–O bond distances of 2.175 and 2.187 Å) with the longer Ca–O bond distance corresponding to the Ca–O bond involved in the H–bond. Noteworthy is the relatively strong interaction of the Ca^{2+} ion with the C atom of the carboxylato group corresponding to a bop value of 0.13 and 0.27 for the isomers **13** and **14**, respectively. Obviously, the Ca^{2+} dication seems to be associated with the carboxylato group in a η^3–bonding mode through the C and the two O donor atoms. This interaction is strongly supported through the electrostatically controlled orientation of the Ca^{2+} dication with respect to the carboxylato group where the higher negative charge resides. The computed molecular electrostatic potential clearly indicates the two possible trajectories for the interaction of Ca^{2+} with the glycolate ligand (Fig. 4). The second trajectory leads to the η^2–O(**O**H),O–(C**O**O$^-$) isomer **15** involving also an asymmetric bonding mode (Ca–O bond distances of 2.027 and 2.286 Å) with the longer Ca–O bond distance corresponding to the Ca–O(H) bond. The association of Ca^{2+} with the glycolate ligand via the η^2–O,O–(C**OO**$^-$) bonding mode results in the lengthening of both the C–O(H) and C–O bonds by about 0.02–0.03 Å with concomitant narrowing of the ∠O=C–O bond angle by about 11°. In the η^2–O(**O**H),O–(C**O**O$^-$) isomer **15** the C–O(H) and C–O bonds are lengthened by 0.044 and 0.080 Å, respectively. The net atomic (natural) charge transferred to Ca^{2+} is 0.72(0.17), 0.79(0.18) and 0.53(0.16) charge units for the isomers **13**, **14** and **15**, respectively. Most of the charge transferred in isomers **13** and **14** comes from the C atom of the coordinated carboxylato group, which acquires a positive net atomic charge of 0.0.40 charge units (compare with the value of 0.13 charge units in the free ligand). In all isomers the negative net atomic charges of the O atoms slightly increase upon coordination.

3.2.2. Infrared spectra

Selected vibrational frequencies in the IR spectra of the $[HOCH_2C(O)OH]Ca^{2+}$ and $[HOCH_2C(O)O]Ca^{+}$ complexes along with the assignment of their normal vibrational modes are listed in the Supporting Information (Table S4). We will only analyze the most characteristic features of the infrared spectra of the complexes in comparison to those of the free ligands. In general terms, all observed shifts of the vibrational frequencies resulted from the association of Ca^{2+} with the glycolic acid conformers and their conjugate bases are in line with both the observed structural and charge distribution changes introduced by the coordination.

In the η^2–O,O–(C**OO**H) coordination **11**, the νC(O)O–H frequency appears shifted 521 cm^{-1} to the red with respect to the free ligand. The opposite is true for the ν(O–H) frequency of the hydroxyl group which is blue-shifted by 130 cm^{-1}. A red shift is also

observed for both the ν(C=O) and ν(C–OH) frequencies found at 129 cm^{-1} and 60 cm^{-1}, respectively. The ν_{as}(O–Ca–O) and ν_{sym}(O–Ca–O) frequencies appear at 344 and 305 cm^{-1}, respectively.

In the η^2–O(**O**H),O–(CO**O**H) coordination **12**, the νC(O)O–H frequency is shifted to the red by 208 cm^{-1} with respect to the free ligand. On the other hand the ν(O–H) frequency of the hydroxyl group is also red-shifted by only 27 cm^{-1}. Contrary to the η^2–O,O–(C**OO**H) coordination mode in the η^2–O(**O**H),O–(CO**O**H) coordination mode the ν(C=O) frequency is blue shifted by 178 cm^{-1}. Moreover, the ν(C–OH) frequency is red shifted by 227 cm^{-1}. The ν_{as}(O–Ca–O) and ν_{sym}(O–Ca–O) frequencies appear at 415 and 285 cm^{-1}, respectively. Obviously, both the ν(C=O) and ν(O–Ca–O) bands could be used as a guide for distinguishing experimentally by IR the bonding mode of glycolic acid with the Ca^{2+} ions.

In the η^2–O,O–(C**OO**$^-$) coordination mode **13** the ν(O–H) frequency of the hydroxyl group is blue-shifted by 343 cm^{-1}. The ν(C=O) frequency is red shifted by 183 cm^{-1} while the ν(C–OH) frequency is blue shifted by 58 cm^{-1}. The ν_{as}(O–Ca–O) and ν_{sym}(O–Ca–O) frequencies appear at 405 and 349 cm^{-1}, respectively. On the other hand, in the η^2–O,O–(C**OO**$^-$) coordination mode **14** the ν(O–H) frequency of the hydroxyl group is blue-shifted by only 29 cm^{-1}, probably because in **14** the H atom is not involved in H-bond formation. The ν(C=O) frequency is red shifted by 164 cm^{-1} while the ν(C–OH) frequency is blue shifted by 100 cm^{-1}. The ν_{as}(O–Ca–O) and ν_{sym}(O–Ca–O) frequencies appear at 420 and 345 cm^{-1}, respectively.

Finally, in the η^2–O(**O**H),O–(C**O**O$^-$) coordination mode **15** the ν(O–H) frequency of the hydroxyl group is red-shifted by only 10 cm^{-1}. On the other hand, the ν(C=O) frequency is blue shifted by 140 cm^{-1} while the ν(C–OH) frequency is red shifted by 133 cm^{-1}. The ν_{as}(O–Ca–O) and ν_{sym}(O–Ca–O) frequencies appear at 423 and 368 cm^{-1}, respectively. Obviously, the ν(C=O) and ν(C–OH) bands could be used as a guide for distinguishing experimentally by IR the η^2–O,O–(C**OO**$^-$) and η^2–O(**O**H),O–(C**O**O$^-$) coordination modes of the glycolate ligand with the Ca^{2+} ions.

3.2.3. NMR spectra

The ^{13}C, ^{17}O, and ^{1}H chemical shifts (δ, ppm) in the NMR spectra of $[HOCH_2C(O)OH]Ca^{2+}$ and $[HOCH_2C(O)O]Ca^{+}$ complexes calculated at the GIAO/B3LYP/6-311 + G(d,p) level of theory using the B3LYP/6-311 + G(d,p) optimized geometries are given in Table 4. The calculated absolute isotropic shielding tensor elements (σ, ppm) are summarized in Supporting Information (Table S5). Notice that the computed NMR spectra of the complexes are predictions as there are no experimental data available so far.

In complex **11** the non-coordinated O(1) is deshielded by 6 ppm with respect to the free ligand. The same is also true for the O(4) donor atom which is deshielded by 34 ppm. Surprisingly O(5) donor atom is shielded by 8 ppm. A strong shielding effect of 32 ppm was also observed for the carboxylic carbon atom C(3). Similarly the C–OH and C(O)OH hydrogen atoms are shielded by 2 and 4 ppm, respectively. In contrast in the η^2–O(**O**H),O–(CO**O**H) coordination **12**, the O(1) and O(5) donor

Table 4
The computed GIAO-B3LYP ^{13}C, ^{17}O and ^{1}H chemical shifts (δ, ppm) of the complexes of glycolic acid conformers and its conjugate bases with Ca^{2+} dications using the 6-311 + G(d,p) basis sets

Compound	$^{17}O(1)$	$^{13}C(2)$	$^{13}C(3)$	$^{17}O(4)$	$^{17}O(5)$	$^{1}H(6)$	$^{1}H(7,8)$	$^{1}H(9)$
13	15.5	71.9	210.3	377.4	202.9	3.4	5.6	12.7
14	64.5	82.5	161.5	485.8	224.8	4.2	5.9	7.7
15	6.9	72.7	163.6	367.0	360.9	1.7	5.1	
16	13.2	73.0	213.8	363.6	387.1	1.0	5.1	
17	59.3	92.1	173.4	451.5	395.9	2.7	5.4	

The calculated absolute ^{13}C, ^{17}O and ^{1}H shielding tensor elements σ^{iso} (σ^{aniso}) for CH_4, H_2O and TMS external reference standards at the same level of theory are 190.4(0.1), 322.6(51.3) and 32.0(9.2), respectively.The calculated absolute ^{40}Ca shielding tensor elements σ^{iso} (σ^{aniso}) for complexes **13**, **14**, **15**, **16**, and **17** are 1291.5(129.7), 1277.6(75.8), 1214.7(121.8), 1210.5(121.8) and 1210.0(164.4), respectively.

atoms are shielded by 47 and 15 ppm, respectively. The same holds true for the non-coordinated O(4) which is much more shielded by 86 ppm. The carboxylic carbon atom C(3) is deshieled by 22 ppm, while C(2) is shielded by 10 ppm. Finally, all H atoms are shielded upon coordination of glycolic acid.

In complex **13** the non-coordinated O(1) is deshielded by 29 ppm with respect to the free ligand. The same is also true for the non-coordinated O(1) in complex **14** which is deshielded by 21 ppm. In contrast, both O(4) and O(5) donor atoms are shielded by 54 and 63 ppm, respectively in complex **13** and 63 and 57 ppm, respectively in complex **14**. The C–OH hydrogen atom is deshielded by 2 ppm in **13** and shielded by 2 ppm in **14**. Finally, in complex **15** the O(1) and O(5) donor atoms are shielded by 25 and 66 ppm, respectively. The same holds true for the non-coordinated O(4) which is much more shielded by 151 ppm. The carboxylic carbon atom C(3) is deshieled by 6 ppm, while C(2) is shielded by 18 ppm. Moreover, the C–OH hydrogen atom is shielded by 4 ppm. Generally, the observed shielding and deshielding effects are compatible with the electron density redistribution reinforced by coordination of the ligands with Ca^{2+}.

3.2.4. Calculated structures, spectroscopic properties and bonding of $[HOCH_2C(O)O]Ca(H_2O)_n$ (n1–4) complexes

The equilibrium structures of $[HOCH_2C(O)O]Ca(H_2O)_n]^+$ ($n = 1–4$) complexes corresponding to global and local minima in the PES computed at the B3LYP/6-311 + G(d,p) level of theory are shown in Fig. 6. In all complexes the glycolato ligand adopts the η^2–O(**O**H),O–(C**O**O$^-$) coordination mode forming with Ca^{2+} ion a five-membered chelate ring. The monoaqua species **16** adopts a pyramidal structure with one of the H atoms of the coordinated water molecule forming a H-bond with the coordinated carboxylato O atom. The O···H separation distance is equal to 2.32 Å.

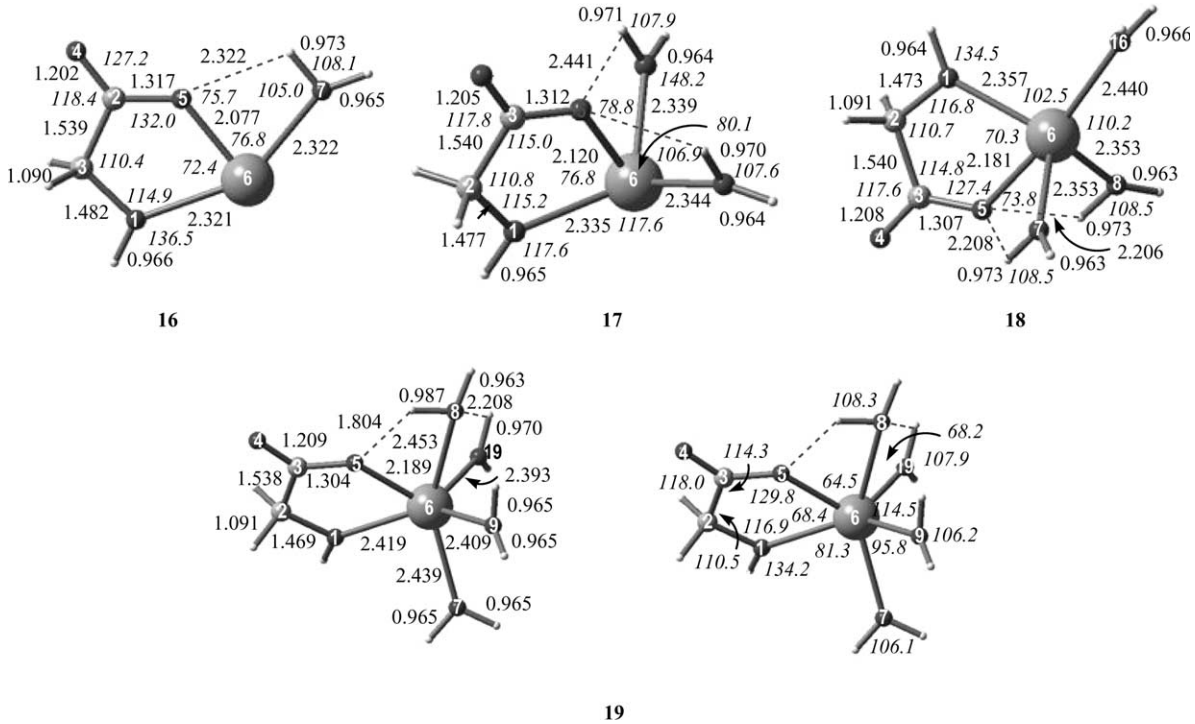

Fig. 6. Equilibrium structures (bond lengths in Å, bond angles in degrees) of $[HOCH_2C(O)O]Ca(H_2O)_n]^+$ ($n = 1–4$) complexes computed at the B3LYP/6-311 + G(d,p) level of theory.

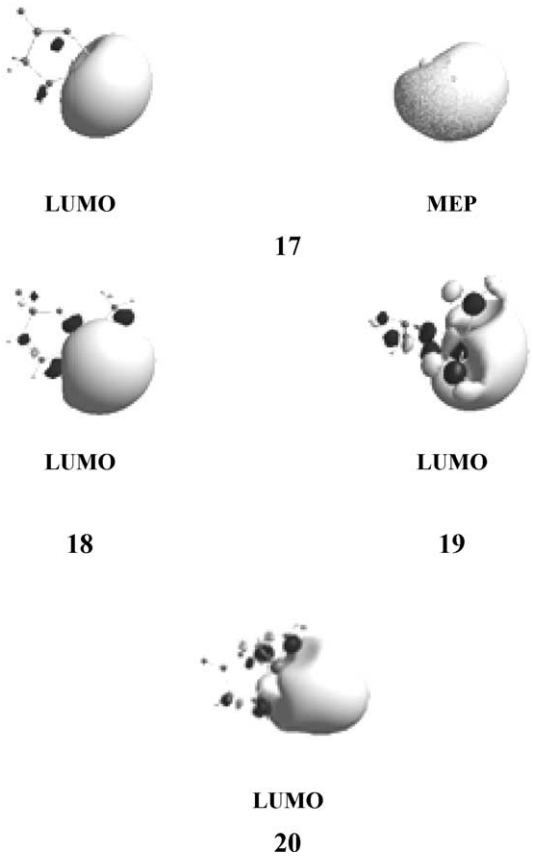

Fig. 7. The LUMO of $[HOCH_2C(O)O]Ca(H_2O)_n]^+$ ($n = 1-4$) complexes along with the MEP of the monoaqua complex computed at the B3LYP/6-311 + G(d,p) level of theory.

The nature of both the LUMO and MEP of the $[HOCH_2C(O)O]Ca^{2+}$ complex shown in Fig. 7 could easily explain the pyramidal structure of **16**. Both have no directional properties, thereby the incoming water ligand is coordinated in such a way in order to favor the H-bond formation with the coordinated carboxylato O atom. The computed binding energy of the water ligand with the $[HOCH_2C(O)O]Ca^{2+}$ fragment is 30.4 kcal mol^{-1} at the B3LYP level of theory. The coordination of the water molecule causes insignificant structural changes on the coordinated glycolato ligand. Thus the two Ca–O coordination bonds are elongated by only about 0.05 Å, all the rest bonds remains essentially unchanged. The same is also true for the charge distribution.

The diaqua species **17** adopts a coordination geometry, which does not correspond to the usual geometries of four-coordinated metal ions. The two water ligands form nearly equivalent coordination bonds with the central Ca^{2+} ion, the Ca–O bond lengths being equal to 2.34 Å. Again the LUMO of **16** (Fig. 7) exhibits a non directional character, thereby the driving force for the orientation of the coordinated water molecules in the coordination sphere are the H-bond formation with the coordinated carboxylato O donor atom bearing the higher negative net atomic charge. Surprisingly this O atom is involved in the formation of H-bonds with both of the coordinated water molecules. The two H-bonds exhibit O···H separation distances of 2.44 and 2.50 Å, respectively. The structural changes introduced by the second water molecule are even smaller, the two Ca–O coordination bonds being elongated by less than 0.04 Å. The computed binding energy of the second water ligand is smaller than that of the first one; the predicted value is 26.8 kcal mol^{-1} at the B3LYP level of theory.

The triaqua species **18** adopts also a coordination geometry, which does not correspond to the usual geometries of five-coordinated metal ions. The two water ligands form nearly equivalent coordination bonds with the central Ca^{2+} ion, the Ca–O bond lengths being equal to 2.35 Å, while the third forms a longer Ca–O coordination bond of 2.44 Å. Only the first two water ligands are involved in H-bond formation with the coordinated carboxylato O donor atom with the two H-bonds exhibiting a similar O···H separation distance of 2.21 Å. The LUMO of **17** (Fig. 7) still exhibits a non directional character, thereby the driving force for the orientation of the coordinated water molecules in the coordination sphere are the H-bond formation with the coordinated carboxylato O donor atom. The structural changes introduced by the third water molecule are larger than to those introduced by the second water molecule, the two Ca-O coordination bonds being elongated by 0.10 and 0.04 Å, respectively. The computed binding energy of the third water ligand is even smaller than that of the second one; the computed value is 22.9 kcal mol^{-1} at the B3LYP level of theory.

Finally, the coordination geometry of the tetraaqua species **19** seems to be very close to a distorted trigonal antiprism, which is not a very common geometry for six-coordinated metal ions. Two of the coordinated water ligands form nearly equivalent coordination bonds with the central Ca^{2+} ion,

the Ca–O bond lengths being equal to 2.40 Å, while the rest two form longer Ca–O coordination bonds of 2.44 and 2.54 Å, respectively. Surprisingly, only one of the water ligands is involved in H-bond formation with the coordinated carboxylato O donor atom, the O···H separation distance being 1.80 Å. The short O···H separation distance illustrates that the H-bond is very strong. Moreover, a second H-bond is formed between the H atom of a coordinated water ligand and the O atom of the water ligand involved in the H-bond formation with the coordinated carboxylato O donor atom. The O···H separation distance in that case is longer (2.21 Å). The LUMO of **18** (Fig. 7) still exhibits a non directional character, thereby the driving force for the orientation of the coordinated water molecules in the coordination sphere are once more the H-bond formation with the coordinated carboxylato O donor atom. The structural changes introduced by the fourth water molecule are even larger than to those introduced by the third water molecule, the two Ca–O coordination bonds being elongated by 0.11 and 0.10 Å, respectively. The computed binding energy of the fourth water ligand is smaller than that of the third one; the computed value is 16.2 kcal mol^{-1} at the B3LYP level of theory. Noteworthy is the trend seen for the incremental binding energy due to the successive addition of water molecules to $[HOCH_2C(O)O]Ca^{2+}$ species. This trend is in accordance with those anticipated from electrostatic considerations. The Ca(II)-water interaction weakens with increasing coordination of the metal. This trend arises from the repulsion of the dipoles between the water ligands and from unfavorable many body interactions. In summary, the electrostatic nature of the Ca(II)-water interactions accounts well for the computed coordination geometries of the cationic (aqua)(glycolato)calcium complexes.

Selected vibrational frequencies in the IR spectra of the $[HOCH_2C(O)O]Ca(H_2O)_n]^+$ ($n = 1–4$) complexes along with the assignment of their normal vibrational modes are listed in the Supporting Information (Table S5). We will only analyze the most characteristic features of the infrared spectra of the complexes in comparison to those of the free of water ligands $[HOCH_2C(O)O]Ca]^+$ complexes. In general terms, upon the successive addition of water molecules to the coordination sphere of the $[HOCH_2C(O)O]Ca]^+$ complex the ν(O–H) frequencies are blue shifted by the increments of 7, 6, 8 and 4 cm^{-1}, respectively, the ν(C=O) frequencies are red shifted by the increments of 14, 15, 7 and 1 cm^{-1} and the ν(C–OH) frequencies are also blue shifted by 42, 10, 11 and 10 cm^{-1}, respectively. All other characteristic bands remain essentially unchanged.

Finally, the ^{13}C, ^{17}O, and ^{1}H chemical shifts (δ, ppm) in the NMR spectra of $[HOCH_2C(O)O]Ca(H_2O)_n]^+$ ($n = 1–4$) complexes calculated at the GIAO/-B3LYP/6-311 + G(d,p) level of theory using the B3LYP/6-311 + G(d,p) optimized geometries are given in Table 5. Notice that the computed NMR spectra of the complexes are predictions as there are no experimental data available so far. In general terms,

Table 5
The computed GIAO-B3LYP ^{13}C, ^{17}O and ^{1}H chemical shifts (δ, ppm) of $[HOCH_2C(O)O]Ca(H_2O)_n]^+$ ($n = 1–4$) complexes using the 6-311 + G(d,p) basis sets

Compound	$^{17}O(1)$	$^{13}C(2)$	$^{13}C(3)$	$^{17}O(4)$	$^{17}O(5)$	$^{17}O(OH_2)$	$^{1}H(OH)$	$^{1}H(CH_2)$	$^{1}H(OH_2)$
18	49.4	86.8	175.1	436.3	357.7	27.7	2.3	5.1	5.3(3.1)
19	46.3	85.4	176.3	426.5	336.4	23.4	2.1	5.0	4.3(2.9)
						24.5			4.5(2.9)
20	44.7	83.6	177.1	416.9	309.5	25.2	1.9	4.9	4.9(2.6)
						10.5			2.6(2.6)
21	39.8	81.7	176.4	408.3	307.2	23.6	1.5	4.7	7.5(2.0)
						14.5			2.4(2.4)
						15.9			2.7(2.5)
						24.8			4.2(2.5)

The calculated absolute ^{13}C, ^{17}O and ^{1}H shielding tensor elements σ^{iso} (σ^{aniso}) for CH_4, H_2O and TMS external reference standards at the same level of theory are 190.4(0.1), 322.6(51.3) and 32.0(9.2), respectively. The calculated absolute ^{40}Ca shielding tensor elements σ^{iso} (σ^{aniso}) for complexes **18**, **19**, **20** and **21** are 1187.0(83.0), 1167.6(29.2), 1145.3(80.9), and 1142.2(79.1), respectively.

upon the successive addition of water molecules to the coordination sphere of the $[HOCH_2C(O)O]Ca]^+$ complex the O(1) is deshielded by the successive increments of about 10, 3, 2 and 5 ppm, respectively. The same holds also true for the O(4) and O(5) which are deshielded by the successive increments of about 15, 10, 10 and 9 ppm and 38, 21, 27 and 2.3 ppm, respectively. The higher deshielding of O(5) could be attributed to the participation of this oxygen atom in the H-bond formation with H atoms of coordinated water ligands. On the other hand the alcoholic C atom is slightly deshielded by successive increments of 5, 1, 2 and 2 ppm while the carboxylic C atom is slightly shielded by successive increments of about 1 ppm.

4. Conclusions

The use of first principles quantum chemical techniques at the B3LYP/6-311 + G(d,p) and CCSD(T)/6-31G(d,p) levels of theory in the exploration of conformational space of glycolic acid and its conjugate base yielded some interesting results. The most stable configuration among the eight possible glycolic acid conformers corresponds to the *E-s-cis*, *s-trans* configuration, while the highest energy *E-s-trans*, *s-cis*conformer was found at 10.88 and 12.17 kcal mol^{-1} higher in energy at the B3LYP/6-311 + G(d,p) and CCSD(T)/6-31G(d,p) levels of theory, respectively. Dissociation of glycolic acid yields either the *s-cis*(*syn*), or *s-trans*(*anti*) conformers of the glycolate anion. The *syn*conformer was found to be the global minimum on the PES, while the *anti* conformer was found to be a local minimum at 14.20 and 16.87 kcal mol^{-1} higher in energy at the B3LYP/6-311 + G(d,p) and CCSD(T)/6-31G(d,p)) levels of theory, respectively. The stabilization of the *syn* conformer is attributed to the intramolecular H-bond formation. The computed B3LYP/6-311 + G(d,p) proton affinity of the *syn* conformer for the protonation process affording the more stable *E-s-cis*, *s-trans* conformer of glycolic acid, in vacuum was found to be 325.35 kcal mol^{-1} (ΔG^0 value). From a methodological point of view, our results confirm the reliability of the integrated computational tool formed by the B3LYP density functional model. This model has subsequently been used to investigate the interaction of Ca^{2+} ions with the glycolic acid conformers and their conjugate bases in vacuum and in the presence of extra water ligands. For the complexes of glycolic acid conformers the η^2–O,O–(C**OO**H) coordination, that is the structure that arises from the coordination of the Ca^{2+} to the carboxylic group, is the global minimum of the PES, while the η^2–O(**O**H),O–(CO**O**H) coordination is a local minimum found at only 1.0 and 1.3 kcal mol^{-1} higher in energy at the B3LYP/6-311 + G(d,p) and CCSD(T)/6-31G(d,p) levels of theory, respectively. Moreover, the two isomers exhibit nearly the same binding affinities, which were found to be 89 and 85 kcal mol^{-1} at the B3LYP/6-311 + G(d,p) and CCSD(T)/6-31G(d,p) levels of theory, respectively. The same holds also true for the complexes of the glycolate anion. The η^2–O,O–(C**OO**$^-$) coordination involving the in the *syn* conformer of the glycolato ligand, is the global minimum, while the η^2–O(**O**H),O–(C**O**O$^-$) one lies at 1.5 and 5.6 kcal mol^{-1} higher in energy at the B3LYP/6-311 + G(d,p) and CCSD(T)/6-31G(d,p) levels of theory, respectively. The other conformer with an η^2–O,O–(C**OO**$^-$) coordination involving *anti* of the glycolato ligand, is less stable by only 0.2 kcal mol^{-1} at both levels of theory. Noteworthy is the trend seen for the incremental binding energy due to the successive addition of water molecules to $[HOCH_2C(O)O]Ca^{2+}$ species; the computed values being 30.4, 26.8, 22.9 and 16.2 kcal mol^{-1} at the B3LYP/6-311 + G(d,p) level of theory for the mono-, di-, tri- and tetraaqua complexes, respectively. This trend arising from the repulsion of the dipoles between the water ligands and from unfavorable many body interactions is in accordance with those anticipated from electrostatic considerations. The Ca(II)-water interaction weakens with increasing coordination of the metal. In summary, the electrostatic nature of the Ca(II)-water interactions accounts well for the computed coordination geometries of the cationic (aqua)(glycolato)calcium complexes. Finally, calculated structures, relative stability and bonding properties of the conformers and their complexes with Ca^{2+} ions are discussed with respect to computed electronic and spectroscopic properties, such as charge density

Table S1
Mulliken and NBO population analysis (net atomic and natural charges, q and bond orbital population, bop) of glycolic acid conformers computed at the B3LYP/6-311 + G(d,p) level of theory

Conformer	*E-s-cis-s-cis* **1**	*Z-s-cis-s-trans* **2TS**	*Z-s-cis-s-trans* **3**	*Z-s-trans-s-cis* **4**	*Z-s-trans-s-trans* **5TS**	*E-s-trans-s-trans* **6**	*E-s-cis-s-cis* **7**	*E-s-trans-s-cis* **8**
q								
O(1)	−0.31(−0.73)	−0.32(−0.73)	−0.30(−0.72)	−0.39(−0.77)	−0.32(−0.72)	−0.30(−0.71)	−0.32(−0.73)	−0.31(−0.71)
C(2)	−0.21(−0.12)	−0.19(−0.13)	−0.15(−0.12)	−0.18(−0.14)	−0.18(−0.12)	−0.24(−0.13)	−0.16(−0.14)	−0.19(−0.14)
C(3)	0.17(0.78)	0.16(0.78)	0.12(0.78)	0.13(0.78)	0.14(0.79)	0.22(0.78)	0.11(0.78)	0.14(0.78)
O(4)	−0.33(−0.61)	−0.30(−0.59)	−0.30(−0.59)	−0.29(−0.58)	−0.31(−0.61)	−0.29(−0.57)	−0.30(−0.58)	−0.26(−0.53)
O(5)	−0.20(−0.68)	−0.27(−0.72)	−0.26(−0.71)	−0.18(−0.67)	−0.18(−0.67)	−0.23(−0.71)	−0.16(−0.67)	−0.18(−0.69)
H(6)	0.25(0.48)	0.26(0.48)	0.26(0.47)	0.28(0.48)	0.25(0.46)	0.25(0.46)	0.26(0.48)	0.25(0.46)
H(7,8)	0.17(0.20)	0.18(0.20)	0.17(0.19)	0.18(0.20)	0.17(0.19)	0.16(0.19)	0.17(0.19)	0.17(0.18)
H(9)	0.27(0.49)	0.29(0.50)	0.28(0.49)	0.27(0.50)	0.27(0.48)	0.27(0.49)	0.24(0.48)	0.23(0.47)
bop								
O(1)–C(2)	0.23	0.20	0.14	0.16	0.13	0.25	0.25	0.25
C(2)–C(3)	0.04	0.21	0.14	0.20	0.21	−0.11	0.13	−0.02
C(3)–O(4)	0.43	0.38	0.40	0.42	0.39	0.46	0.44	0.51
C(3)–O(5)	0.20	0.27	0.22	0.15	0.23	0.28	0.13	0.20
O(5)–H(9)	0.24	0.24	0.23	0.22	0.17	0.25	0.20	0.19
C(2)–H(7,8)	0.40	0.40	0.48	0.41	0.42	0.42	0.41	0.43
O(1)–H(6)	0.28	0.30	0.28	0.21	0.13	0.20	0.28	0.20

Figures in parentheses are the natural charges.

Table S2
Selected harmonic vibrational frequencies (cm^{-1}) and intensities (km mol^{-1}) of glycolic acid conformers and the glycolate anions, calculated at the B3LYP/6-311 + G(d,p) level of theory

Conformer	Vibrational modes					
	νC(O)O–H	ν(O–H)	$\nu_{as}(CH_2)$	$\nu_{sym}(CH_2)$	ν(C=O)	ν(C–O)
s						
E-s-cis-s-trans, **1**	3756(75)[a]	3747(84)	3039(14)	3016(30)	1807(326)	1107(248)
Z-s-cis-s-trans, **2TS**	3828(79)	3764(88)	3050(10)	3026(27)	1830(320)	1153(266)
Z-s-cis-s-trans, **3**	3828(51)	3761(82)	3116(6)	2982(31)	1826(326)	1156(225)
Z-s-trans-s-cis, **4**	3863(60)	3674(159)	3081(11)	3037(18)	1851(338)	1152(125)
E-s-cis-s-trans, **5TS**	3847(41)	3753(72)	3032(18)	3002(30)	1806(341)	1167(347)
E-s-cis-s-trans, **6**	3852(51)	3767(76)	3023(22)	2994(35)	1851(330)	1097(378)
E-s-cis-s-trans, **7**	3794(60)	3722(88)	3008(21)	2987(41)	1842(267)	1114(180)
E-s-cis-s-trans, **8**	3852(53)	3795(40)	2997(27)	2963(51)	1882(278)	1095(168)
s-cis, **9**		3461(246)	3010(77)	2984(96)	1682(540)	1057(130)
s-trans, **10**		3812(0)	3006(81)	2972(86)	1683(631)	1023(106)

[a] Figures in parentheses are the intensities.

Table S3
Mulliken and NBO population analysis (net atomic and natural charges, **q**, bond orbital population, bop and natural electron configuration, *nec*, of Ca) of $[HOCH_2C(O)OH]Ca^{2+}$ and $[HOCH_2C(O)O]Ca^{2+}$ complexes computed at the B3LYP/6-311 + G(d,p) level of theory

Complex	**13**	**14**	**15**	**16**	**17**
q					
O(1)	−0.37(−0.76)	−0.46(−0.89)	−0.28(−0.71)	−0.29(−0.71)	−0.48(−0.90)
C(2)	−0.14(−0.14)	−0.27(−0.14)	−0.22(−0.13)	−0.19(−0.13)	−0.28(−0.13)
C(3)	0.34(0.86)	0.26(0.78)	0.40(0.78)	0.41(0.79)	0.23(0.76)
O(4)	−0.34(−0.74)	−0.08(−0.39)	−0.40(−0.84)	−0.42(−0.85)	−0.24(−0.53)
O(5)	−0.33(−0.78)	−0.46(−0.92)	−0.44(−0.86)	−0.37(−0.81)	−0.46(−1.00)
H(6)	0.35(0.53)	0.37(0.55)	0.26(0.48)	0.27(0.48)	0.32(0.52)
H(7,8)	0.25(0.26)	0.28(0.27)	0.38(0.22)	0.19(0.21)	0.22(0.22)
H(9)	0.39(0.58)	0.38(0.56)			
Ca	1.60(1.92)	1.69(1.93)	1.28(1.83)	1.21(1.82)	1.47(1.84)
bop					
O(1)–C(2)	0.08	0.08	0.33	0.13	0.05
C(2)–C(3)	0.33	0.17	−1.08	−2.45	0.29
C(3) − O(4)	0.27	0.45	−0.10	−0.08	0.46
C(3)–O(5)	−0.05	0.01	0.02	−0.01	0.21
O(5)–H(9)	0.39	0.24	0.16	0.17	0.17
C(2)–H(7,8)	0.42	0.43	0.38	0.41	0.43
O(1)–H(6)	0.24	0.27	0.29	0.17	0.22
Ca–O(1)		0.08			0.07
Ca–O(3)	0.06		0.13	0.27	
Ca–O(4)	0.16		0.15	0.15	
Ca–O(5)	0.06	0.08	0.16	0.17	0.17
nec					
Ca	$4s^{0.03}3d^{0.05}$	$4s^{0.02}3d^{0.05}$	$4s^{0.05}3d^{0.12}$	$4s^{0.06}3d^{0.13}$	$4s^{0.03}3d^{0.13}$

Figures in parentheses are the natural charges.

Table S4
Selected harmonic vibrational frequencies (cm^{-1}) and intensities (km mol^{-1}) of the $[HOCH_2C(O)OH]Ca^{2+}$ and $[HOCH_2C(O)O]Ca^{+}$ complexes calculated at the B3LYP/6-311 + G(d,p) level of theory

Compound	Vibrational modes								
	νC(O)**O**–**H**	ν(O–H)	$\nu_{as}(CH_2)$	$\nu_{sym}(CH_2)$	ν(C=O)	ν(C(O)–OH)	ν(C–OH)	ν_{as}(O–Ca–O)	ν_{sym}(O–Ca–O)
13	3342(75)	3804(489)	3034(6)	2999(37)	1722(442)	1358(248)	1092(248)	344(67)	305(34)
14	3639(247)	3726(230)	3123(13)	3067(17)	1984(242)	1080(411)	940(49)	415(37)	285(25)
15		3804(66)	3027(2)	3008(27)	1499(105)		1115(166)	405(68)	349(40)
					1479(102)				
16		3841(91)	3014(7)	2989(27)	1519(116)		1123(109)	420(30)	345(43)
					1480(209)				
17		3802(118)	3146(6)	3083(3)	1823(462)		890(123)	423(47)	368(34)

Figures in parentheses are the intensities.

Table S5
Selected harmonic vibrational frequencies (cm^{-1}) and intensities (km mol^{-1}) of the $[HOCH_2C(O)O]Ca(H_2O)_n]^{+}$ ($n = 1–4$ complexes calculated at the B3LYP/6-311 + G(d,p) level of theory

Compound	Vibrational modes								
	$\nu_{as}(OH_2)$	ν(O–H)	$\nu_{s}(OH_2)$	$\nu_{as}(CH_2)$	$\nu_{sym}(CH_2)$	ν(C=O)	ν(C–OH)	ν_{as}(O–Ca–O)	ν_{sym}(O–Ca–O)
18	3859(247)	3809(230)	3703(13)	3141(17)	3080(242)	1809(411)	932(49)	405(37)	379(25)
								324(36)	236(9)
19	3866(234)	3815(98)	3733(98)	3134(2)	3075(5)	1794(539)	942(21)	394(17)	388(114)
								338(10)	233(5)
20	3876(190)	3823(84)	3692(246)	3129(6)	3072(8)	1787(579)	953(33)	381(13)	360(22)
								321(5)	239(5)
21	3884(186)	3827(61)	3745(548)	3123(4)	3068(10)	1786(597)	963(36)	373(102)	370(187)
								336(20)	247(4)

Figures in parentheses are the intensities.

distribution, harmonic vibrational frequencies and NMR chemical shifts.

5. Supporting information available

Tables S1 and S3 showing the Mulliken and NBO population analysis (net atomic and natural charges, q and bond orbital population, bop) of glycolic acid conformers and the $[HOCH_2C(O)OH]Ca^{2+}$ and $[HOCH_2C(O)O]Ca^{2+}$ complexes computed at the B3LYP/6-311 + G(d,p) level of theory. Tables S2, S4 and S5, showing selected harmonic vibrational frequencies (cm^{-1}) and intensities (km mol^{-1}) of glycolic acid conformers, the glycolate ligands, the $[HOCH_2C(O)OH]Ca^{2+}$, $[HOCH_2C(O)O]Ca^{2+}$ and $[HOCH_2C(O)O]Ca(H_2O)_n]^{+}$ ($n = 1–4$) complexes calculated at the B3LYP/6-311 + G(d,p) level of theory.

References

[1] G. Bojesen, T. Breindhal, U.N. Andersen, Org. Mass Spectrom. 28 (1993) 1448.
[2] J.S. Klassen, S.G. Anderson, A.T. Blades, P. Kebarle, J. Phys. Chem. 100 (1996) 14218.
[3] S. Bouchonet, Y. Hoppilliard, Org. Mass Spectrom. 27 (1992) 71. (b) S. Bouchonet, J.P. Flament, Y. Hoppilliard, Rapid Commun. Mass Spectrom. 7 (1993) 470.
[4] F. Jensen, J. Am. Chem. Soc. 114 (1992) 9533.
[5] S. Hoyau, G. Ohanessian, Chem. Eur. J. 4 (1998) 1561.
[6] T. Wyttenbach, M. Witt, M.T. Bowers, Int. J. Mass Spectrom. 182–183 (2001) 243.

[7] S. Pulkkinen, M. Noguera, L. Rodríguez-Santiago, M. Sodupe, J. Bertran, Chem. Eur. J. 6 (2000) 4393.
[8] E.F. Strittmatter, A.S. Lemoff, E.R. Williams, J. Phys. Chem. A 104 (2000) 9793.
[9] S. Hoyau, G. Ohanessian, J. Am. Chem. 119 (1997) 2016.
[10] J. Bertran, L. Rodríguez-Santiago, M. Sodupe, J. Phys.Chem. B 103 (1999) 2310.
[11] L. Rulíšek, Z. Havlas, J. Am. Chem. Soc. 122 (2000) 10428.
[12] M. Remko, B.M. Rode, Chem. Phys. Lett. 316 (2001) 489.
[13] W.J. Hehre, L. Radom, P.v.R. Schleyer, J.A. Pople, Ab initio Molecular Orbital Theory, Wiley, New York, 1986.
[14] R.G. Parr, W. Yang, Density Functional Theory of Atoms and Molecules, Oxford University Press, New York, 1989.
[15] M.J. Frisch, G.W. Trucks, H.B. Schlegel, G.E. Scuseria, M.A. Robb, J.R. Cheeseman, V.G. Zakrzewski, J.A. Montgomery, Jr., R.E. Stratmann, J.C. Burant, S. Dapprich, J.M. Millam, A.D. Daniels, K.N. Kudin, M.C. Strain, O. Farkas, J. Tomasi, V. Barone, M. Cossi, R. Cammi, B. Mennucci, C. Pomelli, C. Adamo, S. Clifford, J. Ochterski, G.A. Petersson, P.Y. Ayala, Q. Cui, K. Morokuma, D.K. Malick, A.D. Rabuck, K. Raghavachari, J.B. Foresman, J. Cioslowski, J.V. Ortiz, A.G. Baboul, B.B. Stefanov, G. Liu, A. Liashenko, P. Piskorz, I. Komaromi, R. Gomperts, R.L. Martin, D.J. Fox, T. Keith, M.A. Al-Laham, C.Y. Peng, A. Nanayakkara, C. Gonzalez, M. Challacombe, P.M.W. Gill, B. Johnson, W. Chen, M.W. Wong, J.L. Andres, C. Gonzalez, M. Head-Gordon, E.S. Replogle, J.A. Pople, GAUSSIAN 98, Revision A.7, Gaussian, Inc., Pittsburgh PA, 1998
[16] H.B. Schlegel, J. Comput. Chem. 3 (1982) 214.
[17] R. Ditchfield, Mol. Phys. 27 (1974) 789. (b) J. Gauss, J. Chem. Phys. 99 (1993) 3629.
[18] G. Jeffrey, An Introduction to Hydrogen Bonding, Oxford University Press, New York, 1997. (b) R.F.W. Bader, Chem. Rev., 91, 1991, pp. 893.
[19] C.E. Blom, A. Bauder, J. Am. Chem. Soc. 104 (1982) 2993.
[20] M.D. Liptak, G.C. Shields, J. Am. Chem. Soc. 123 (2001) 7314.
[21] R.G. Parr, R.G. Pearson, J. Am. Chem. Soc. 105 (1983) 7512. (b) R.G. Pearson, J. Chem. Educ. 64 (1987) 561. (c) R.G. Pearson, Acc. Chem. Res. 26 (1992) 250.
[22] L.L.G. Justino, M.L. Ramos, M.M. Caldeira, V.M.S. Gil, Inorg. Chim. Acta. 311 (2000) 119.